J Appl Electrochem (2010) 40:2023–2032
DOI 10.1007/s10800-010-0182-y

ORIGINAL PAPER

Electrocoagulation studies on removal of cadmium using magnesium electrode

Subramanyan Vasudevan · Jothinathan Lakshmi · Murthy Packiyam

Received: 29 December 2009 / Accepted: 18 July 2010 / Published online: 27 July 2010

Abstract The removal of cadmium from aqueous solution was carried out by electrocoagulation using magnesium as anode and stainless steel as cathode. Various operating parameters on the removal efficiency of cadmium were investigated, such as initial cadmium ion concentration, initial pH, current density and temperature. The optimum removal efficiency of 98.6% was achieved at a current density of 0.2 A dm^{-2} at a pH of 7.0. The experimental data were tested against different adsorption isotherm models for describing the electrocoagulation process. The adsorption of cadmium preferably fitting the Langmuir adsorption isotherm suggests monolayer coverage of adsorbed molecules. First and second-order rate equations were applied to study adsorption kinetics. The adsorption process follows second order kinetics model with good correlation. Temperature studies showed that adsorption was endothermic and spontaneous in nature.

Keywords Electrocoagulation · Cadmium removal · Adsorption · Kinetics and isotherms

1 Introduction

It is generally known that heavy metals present in surface waters are awfully dangerous to environmental and human health because they are not biodegradable and must be removed to prevent their accumulation. Cadmium is one of the most toxic non-essential heavy metals present in the environment, even at low concentrations. Elevated level of cadmium ions arise from a variety of sources such as wastewater from metal plating industries, nickel–cadmium batteries, phosphate fertilizer, mining, pigments, stabilizers, alloys, petroleum refining, welding and pulp industries [1–3]. Cadmium poisoning includes kidney damage [4], lung insufficiency, cancer; it changes the constitution of bone, liver and blood [5]. Cadmium accumulated in the rice crops, it developed Itai-Itai disease and renal abnormalities including proteinuria and glucosuria. Cadmium containing compounds are known as carcinogens [6, 7]. The drinking water guideline value recommended by World Health Organization (WHO) is 0.005 mg L^{-1} [8].

Conventional methods for removing cadmium from water include ion exchange, reverse osmosis, co-precipitation, coagulation, complexation, solvent extraction, electrochemical treatment and adsorption [9–25]. Physical methods like ion exchange, reverse osmosis and electrodialysis have proven to be either too expensive or inefficient to remove cadmium from water. At present, chemical treatments are not used due to disadvantages like high costs of maintenance, problems of sludge handling and its disposal, and neutralization of the effluent [26]. The cadmium removal from water by adsorption using different materials has also been explored. The major disadvantages of this studied adsorbent are low efficiency and high cost. Recent research has demonstrated that electrocoagulation offers an attractive alternative to above-mentioned traditional methods for treating water [27]. In this process anodic dissolution of metal electrode takes place with the evolution of hydrogen gas at the cathode [28]. Electrochemically generated metallic ions from the anode can undergo hydrolysis to produce a series of activated intermediates that are able to destabilize the finely dispersed particles present in

S. Vasudevan (✉) · J. Lakshmi
Central Electrochemical Research Institute (CSIR), Karaikudi 630 006, India
e-mail: vasudevan65@gmail.com

M. Packiyam
Urumu Dhanalakshmi College, Trichy, India

the water to be treated. The destabilized particles then aggregate to form flocks as outlined below,

(i) When magnesium and stainless steel is used as the anode and cathode respectively, the reactions are as follows:

At the cathode: $2H_2O + 2e^- \rightarrow H_2\,(g) + 2OH^-$ (1)

At the anode: $Mg \rightarrow Mg^{2+} + 2e^-$ (2)

In the solution: $Mg^{2+}\,(aq) + 2H_2O \rightarrow Mg(OH)_2 + 2H^+\,(aq)$ (3)

(ii) When aluminium and stainless steel is used as the anode and cathode respectively, the reactions are as follows:

At the cathode: $2H_2O + 2e^- \rightarrow H_2\,(g) + 2OH^-$ (4)

At the anode: $Al \rightarrow Al^{3+} + 3e^-$ (5)

In the solution: $Al^{3+}\,(aq) + 3H_2O \rightarrow Al(OH)_3 + 3H^+\,(aq)$ (6)

The advantages of electrocoagulation include high particulate removal efficiency, a compact treatment facility, relatively low cost, and the possibility of complete automation. This method is characterized by reduced sludge production, a minimum requirement of chemicals and ease of operation [25, 29, 30]. Apart from the above, the main disadvantage in case of aluminum electrode is the residual aluminum (The USEPA guidelines suggest maximum contamination is 0.05–0.2 mg L^{-1}) present in the treated water due to cathodic dissolution. This will create health problems like cancer. In the case of magnesium electrodes, there is no such disadvantage like aluminum electrodes. Because the USEPA guidelines suggest maximum guidelines value of magnesium in water is 30 mg L^{-1}.

This article presents the results of the laboratory scale studies on the removal of cadmium using magnesium and stainless steel as anode and cathode respectively by electrocoagulation process. To optimize the maximum removal efficiency of cadmium, different parameters like effect of initial concentration, effect of temperature, pH and effect of current density were studied. In doing so, the equilibrium adsorption behavior is analyzed by fitting models of Langmuir, Freundlich and D-R. Adsorption kinetics of electrocoagulants is analyzed using first and second order kinetic models. Activation energy is evaluated to study the nature of adsorption.

2 Materials and methods

2.1 Experimental apparatus and procedures

Figure 1 shows the electrolytic cell consisted of a 1.0-L Plexiglas vessel that was fitted with a polycarbonate cell

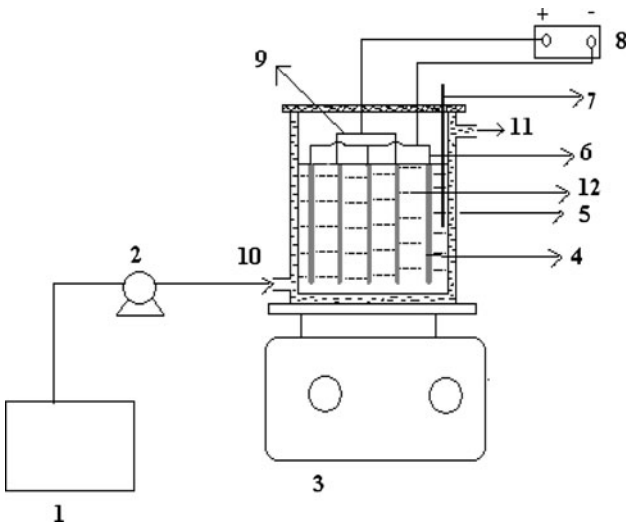

Fig. 1 Laboratory scale cell assembly: *1* water feed tank, *2* pump, *3* magnetic stirrer, *4* cell, *5* thermostatic water, *6* stainless steel cathode, *7* pH sensor and thermometer, *8* DC source, *9* magnesium anode, *10* inlet of thermostatic water, *11* outlet of thermostatic water, *12* electrolyte containing cadmium

cover with slots to introduce the anode, cathode, pH sensor, a thermometer and electrolytes. Magnesium sheet (Alfa Aesar) of surface area (0.02 m^2) acted as the anode. The cathodes were stainless steel (commercial grade) sheets of the same size as the anode is placed at an interelectrode distance of 0.005 m. The temperature of the electrolyte was controlled to the desired value with a variation of ±2 K by adjusting the rate of flow of thermostatically controlled water through an external glass-cooling spiral. A regulated direct current (DC) was supplied from a rectifier (10 A, 0–25 V; Aplab model).

Cadmium nitrate $Cd(NO_3)_2{\cdot}4H_2O$ (Analar Reagent) was dissolved in distilled water for the required concentration. In all the experiments 20 mg L^{-1} of cadmium was used. The solution of 0.90 L was used for each experiment as the electrolyte. The pH of the electrolyte was adjusted, if required, with 1 mol L^{-1} HCl or NaOH solutions before adsorption experiments. To examine the effect of co-existing ions, for the removal of cadmium, Analar Grade sodium salts of carbonate, phosphate, silicate and arsenate were added to the electrolyte for required concentrations.

2.2 Analytical methods

The concentration of cadmium was determined using UV–visible Spectrophotometer with cadmium kits (MERCK, Pharo 300, Germany). The SEM and EDAX of cadmium adsorbed magnesium hydroxide coagulant were analyzed with a Scanning Electron Microscope (SEM) made by Hitachi (model s-3000h). The Fourier transform infrared spectrum of magnesium hydroxide was obtained

using Nexus 670 FTIR spectrometer made by Thermo Electron Corporation, USA. The XRD for magnesium hydroxide coagulant was analyzed by X-ray diffractometer made by JEOL X-ray diffractometer (Type—JEOL, Japan).

3 Results and discussion

3.1 Effect of current density

It has been established that the current density is an important operating factor influencing the performance of electrochemical process which determines the coagulant dosage. The coagulant or amount of adsorbent [$Mg(OH)_2$] was determined from the Faraday law,

$$E_c = ItM/ZF \quad (7)$$

where I is current in (A), t is the time (s), M is the molecular weight, Z is the number of electron involved, and F is the faraday constant (96485.3 C mol^{-1}). To examine the effects of current density, a series of experiments were carried out using 20 mg L^{-1} cadmium-containing electrolyte, at pH 7.0, with the current density being varied from 0.1 to 0.5 A dm^{-2}. The removal efficiencies of cadmium are 97.2, 98.6, 98.8, 99.1 and 99.36% for current densities of 0.1, 0.2, 0.3, 0.4 and 0.5 A dm^{-2} respectively. From results, it is found that, beyond the current density of 0.2 A dm^{-2} the removal efficiencies remain almost constant for higher current densities. Hence, further experiments were carried out at a current density of 0.2 A dm^{-2}. At a high current density, the extent of anodic dissolution of magnesium increases, resulting in a greater amount of precipitate and removal of cadmium, which indicates that the adsorption depends up on the availability of binding sites for cadmium.

3.2 Effect of pH

The pH of the aqueous solution is an important variable, which can affect the extent of adsorption because it influences the metal speciation in aqueous solution as well as the surface properties of the adsorbent. To explain this effect, a series of experiments were carried out using 20 mg L^{-1} cadmium containing solutions, with an initial pH varying in the range 4 to 9. The removal efficiency of cadmium was increased with increasing the pH up to 7. When the pH is above 7, removal efficiency should be slightly decreased. It is found that the maximum removal efficiency for the removal of cadmium is 98.6% at pH 7 and the minimum efficiency is 86.2% at pH 4.

The decrease of removal efficiency at more acidic and alkaline pH was observed by many investigators and was attributed to an amphoteric behavior of $Al(OH)_3$ which leads to soluble Al^{3+} cations (at acidic pH) and to monomeric anions $Al(OH)^{4-}$ (at alkaline pH). It is well known that these soluble species are not useful for water treatment. When the initial pH was kept in neutral, all the aluminum produced at the anode formed polymeric species ($Al_{13}O_4(OH)_{24}{}^{7+}$) and precipitated $Al(OH)_3$ leading to more removal efficiency. In the present study, the electrolyte pH was maintained in neutral, so the formation of $Mg(OH)_2$ is more predominant (like aluminium), leading to greater removal efficiency.

3.3 Effect of initial cadmium concentration

To study the effect of initial concentration, experiments were conducted at varying initial concentrations from 10 to 50 mg L^{-1}. The results are illustrated in Fig. 2. From the results it can be seen that the adsorption of cadmium is increased with an increase in cadmium concentration and remains constant after equilibrium time. The equilibrium time was 45 min for all of the concentrations studied (10–50 mg L^{-1}). The amount of cadmium adsorbed (q_e) increased from 9.83 to 44.26 mg g^{-1} as the concentration was increased from 10 to 50 mg L^{-1}. The figure also shows that the adsorption is the rapid in the initial stages and gradually decreases with progress of adsorption this is because of the great number of sites available for the sorption operation and adsorption equilibrium were then gradually achieved. The plots are single, smooth and continuous curves leading to saturation, suggesting the possible monolayer coverage to cadmium on the surface of the adsorbent [31, 32].

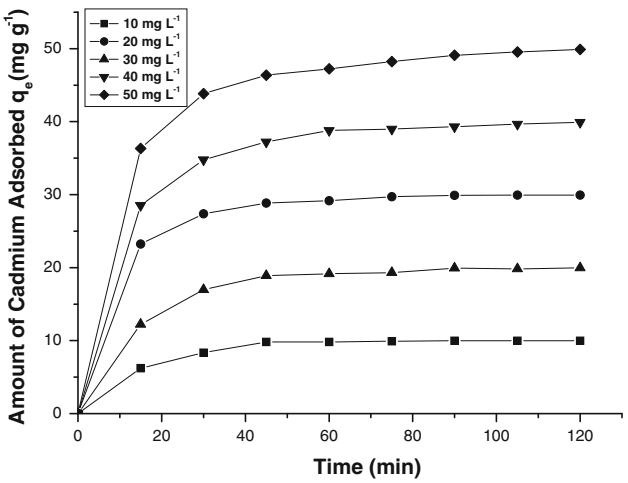

Fig. 2 Effect of agitation time and amount of a cadmium adsorbed: **a** at a current density of 0.2 A dm^{-2}, **b** pH of 7.0 and **c** temperature of 303 K

3.4 Effect of coexisting anions

3.4.1 Carbonate

Effect of carbonate on cadmium removal was evaluated by increasing the carbonate concentration from 0 to 250 mg L^{-1} in the electrolyte. The removal efficiencies are 98.6, 98.2, 58.2, 40.6, 18, and 11% for the carbonate ion concentration of 0, 2, 5, 65, 150 and 250 mg L^{-1} respectively. From the results it is found that the removal efficiency of the cadmium is not affected by the presence of carbonate below 2 mg L^{-1}. Significant reduction in removal efficiency was observed above 5 mg L^{-1} of carbonate concentration is due to the passivation of anode resulting, the hindering of the dissolution process of anode.

3.4.2 Phosphate

The concentration of phosphate ion was increased from 0 to 50 mg L^{-1}, the contaminant range of phosphate in the ground water. The removal efficiency for cadmium was 98.6, 98.5, 55, 41.7 and 38% for 0, 2, 5, 25 and 50 mg L^{-1} of phosphate ion respectively. There is no change in removal efficiency of cadmium below 2 mg L^{-1} of phosphate in the water. At higher concentrations (at and above 5 mg L^{-1}) of phosphate, the removal efficiency decreases drastically. This is due to the preferential adsorption of phosphate over cadmium as the concentration of phosphate increase.

3.4.3 Arsenic

From the results it is found that the efficiency decreased from 98.6 to 35% by increasing the concentration of arsenate from 0 to 5 mg L^{-1}. This is due to the preferential adsorption of arsenic over cadmium as the concentration of arsenate increases. So, when arsenic ions are present in the water to be treated arsenic ions compete greatly with cadmium ions for the binding sites.

3.4.4 Silicate

From the results it is found that no significant change in cadmium removal was observed, when the silicate concentration was increased from 0 to 2 mg L^{-1}. The respective efficiencies for 0, 2, 5, 10 and 15 mg L^{-1} of silicate are 98.6, 84.8, 77, 63 and 49%. The removal of cadmium decreased with increasing silicate concentration from 0 to 15 mg L^{-1}. In addition to preferential adsorption, silicate can interact with magnesium hydroxide to form soluble and highly dispersed colloids that are not removed by normal filtration.

3.5 Adsorption kinetics

The adsorption of cadmium is analyzed using Lagergren rate equation. The first order Lagergren model is [33, 34].

$$dq/dt = k_1(q_e - q_t) \quad (8)$$

where, q_t is the amount of cadmium adsorbed on the adsorbent at time t (min) and k_1 (min^{-1}) is the rate constant of first order adsorption. The integrated form of the above equation with the boundary conditions t = 0 to >0 (q = 0 to >0) is rearranged to obtain the following time dependence function,

$$\log(q_e - q_t) = \log(q_e) - k_1 t/2.303 \quad (9)$$

where q_e is the amount of cadmium adsorbed at equilibrium. The q_e and rate constant (k_1) were calculated from the slope of the plots of $\log(q_e - q_t)$ versus time (t) (figure not shown). It was found that the calculated q_e value do not agrees with the experimental q_e values.

The second order kinetic model is expressed as [35]

$$dq/dt = k_2(q_e - q_t)^2 \quad (10)$$

where k_2 is the rate constant of second order adsorption. The integrated form of Eq. 10 with the boundary condition t = 0 to >0 (q = 0 to >0) is

$$1/(q_e - q_t) = 1/q_e + k_2 t \quad (11)$$

Equation 11 can be rearranged and linearized as,

$$t/q_t = 1/k_2 q_e^2 + t/q_e \quad (12)$$

The plot t/q_t versus time (t) (Fig. 3) shows the straight line. The second order kinetic values of q_e and k_2 were calculated from the slope and intercept of the plots t/q_t vs. t.

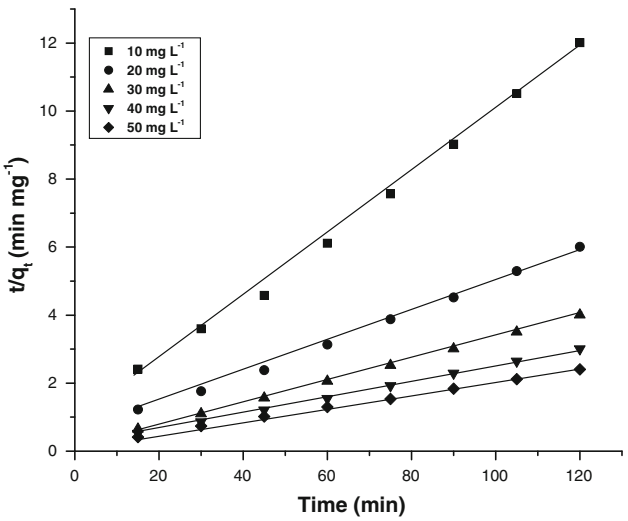

Fig. 3 Second order kinetic model plot of different concentrations of cadmium: **a** at current density of 0.2 A dm^{-2}, **b** temperature of 303 K and **c** pH of 7.00

Table 1 Comparison between the experimental and calculated q_e values for different initial cadmium concentrations in first and second order adsorption kinetic at temperature 305 K and pH 7

Concentration (mg L^{-1})	q_e (exp)	First order adsorption			Second order adsorption		
		q_e (Cal)	$K_1 \times 10^4$ (min mg^{-1})	R^2	q_e (Cal)	$K_2 \times 10^4$ (min mg^{-1})	R^2
10	9.83	45.89	−0.0028	0.0768	7.559	2.492	0.9926
20	18.89	45.24	−0.0077	0.4568	18.101	5.284	0.9978
30	27.36	45.28	−0.0079	0.5032	28.485	7.498	0.9997
40	37.22	45.16	−0.0179	0.7863	36.957	3.774	0.9997
50	44.26	45.08	−0.0280	0.8332	45.082	2.232	0.9992

Table 1 depict the computed results obtained from first and second order kinetic model. The calculated q_e values agree well with the experimental q_e values for second order kinetics model better than for first order kinetics model. These results indicate that the adsorption system belongs to the second order kinetic model.

3.6 Adsorption isotherm

The adsorption capacity of the adsorbent has been tested using Freundlich, Langmuir and Dubinin–Radushkevich isotherms. These models have been widely used to describe the behavior of adsorbent-adsorbate couples. To determine the isotherms, the initial pH was kept at 7 and the concentration of cadmium used was in the range of 10–50 mg L^{-1}.

3.6.1 Freundlich isotherm

The Freundlich isotherm is an empirical model relates the adsorption intensity of the sorbent towards adsorbent. The isotherm is adopted to describe reversible adsorption and not restricted to monolayer formation. The mathematical expression of the Freundlich model can be written as [36]

$$q_e = KC^n \tag{13}$$

Equation 13 can be linearized in logarithmic form and the Freundlich constants can be determined as follows [37]

$$\log q_e = \log k_f + n\log C_e \tag{14}$$

where, k_f is the Freundlich constant related to adsorption capacity, n is the energy or intensity of adsorption, C_e is the equilibrium concentration of cadmium. To determine the isotherms, the cadmium concentration used was 10–50 mg L^{-1} and at an initial pH 7. The Freundlich constants k_f and n values are 1.1147 (mg g^{-1}) and 1.0550 (L mg^{-1}) respectively. It has been reported that values of n lying between 0 and 1 indicate favorable adsorption. From the analysis of the results it is found that the Freundlich plots fit satisfactorily with the experimental data obtained in the present study.

3.6.2 Langmuir isotherm

The linearized form of Langmuir adsorption isotherm model is [38]

$$C_e/q_e = 1/q_o b + C_e/q_o \tag{15}$$

where C_e is the concentration of the cadmium solution (mg L^{-1}) at equilibrium, q_o is the adsorption capacity (Langmuir constant) and b is the energy of adsorption. Figure 4 shows the Langmuir plot with experimental data. Langmuir plot is a better fit with the experimental data compare to Freundlich plots. The value of the adsorption capacity q_o as found to be 427.350 mg g^{-1} which is higher than that of other adsorbents studied. The essential characteristics of the Langmuir isotherm can be expressed as the dimensionless constant R_L [39]

$$R_L = 1/(1 + bC_o) \tag{16}$$

where R_L is the equilibrium constant it indicates the type of adsorption, C_o is the initial cadmium concentration and b is the Langmuir constant. It is well known that the R_L values indicate the type of isotherm: irreversible ($R_L = 0$),

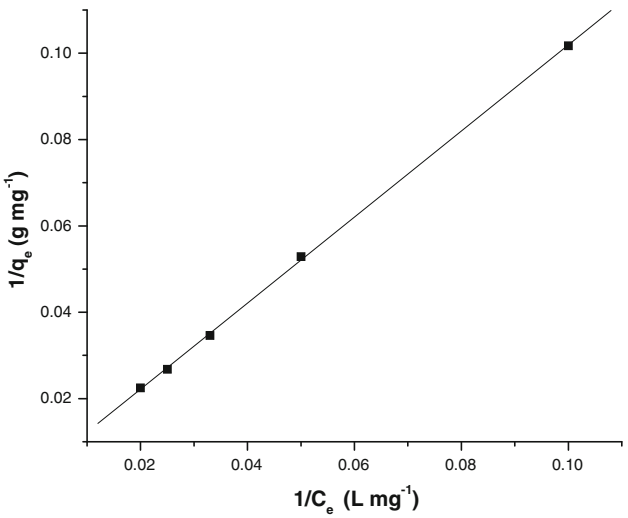

Fig. 4 Langmuir plot for adsorption of cadmium: **a** at pH of 7.0, **b** current density of 0.2 A dm^{-2} and **c** temperature of 303 K

Table 2 Constant parameters and correlation co-efficient calculated for different adsorption isotherm models at room temperature for cadmium adsorption at 20 mg L^{-1}

Isotherm	Constants			
	Q_o (mg g^{-1})	B (L mg^{-1})	R_L	R^2
Langmuir	427.350	0.00235	0.9551 (10 mg L^{-1})	0.9996
			0.9770 (20 mg L^{-1})	
			0.9341 (30 mg L^{-1})	
			0.9141 (40 mg L^{-1})	
			0.8948 (50 mg L^{-1})	
	K_f (mg g^{-1})		n (L mg^{-1})	R^2
Freundlich	1.1147		1.0550	0.9856
	Q_s ($\times 10^3$ mol g^{-1})	B ($\times 10^3$ mol^2 kJ^{-2})	E (kJ mol^{-1})	R^2
D–R	0.2698	0.1953	0.2056	0.8653

favorable ($0 < R_L < 1$), linear ($R_L = 1$) or unfavorable ($R_L > 1$). In present study, the R_L values were found to be between 0 and 1 for all the concentration of cadmium studied (10–50 mg L^{-1}). The results are presented in Table 2.

3.6.3 Dubinin–Radushkevich (D–R) isotherm

Dubinin and Radushkevich have proposed another isotherm which can be used to analyze the equilibrium data. It is not based on the assumption of homogeneous surface or constant adsorption potential, but it is applied to estimate the mean free energy of adsorption (E). This model is given by

$$q_e = q_s \exp\left(-B\varepsilon^2\right) \quad (17)$$

where ε is Polanyi potential, equal to RT ln(1 + 1/C_e), B is related to the free energy of sorption and q_s is the Dubinin–Radushkevich (D–R) isotherm constant [40]. The linearized form is

$$\ln q_e = \ln q_s - 2B\ RT \ln[1 + 1/C_e] \quad (18)$$

The isotherm constants of q_s and B are obtained from the intercept and slope of the plot of ln q_e vs. ε^2 [41]. The constant B gives the mean free energy of adsorption per molecule of the adsorbate when it is transferred from the solid from infinity in the solution and the relation is given as

$$E = [1/\sqrt{2B}] \quad (19)$$

The magnitude of E is useful for estimating the type of adsorption process. It was found to be 0.2056 kJ mol^{-1}, which is too much smaller then the energy range of adsorption reaction, 8–16 kJ mol^{-1} [42]. So the type of adsorption of cadmium on magnesium was defined as chemical adsorption.

The correlation coefficient values of different isotherm models are listed in Table 2. The Langmuir isotherm model has a higher regression coefficient ($R^2 = 0.999$) when compared to the other models. The value of R_L for the Langmuir isotherm was calculated from 0 to 1, indicating the favorable adsorption of cadmium.

3.7 Effect of temperature

The amount of cadmium adsorbed on the adsorbent increases by increasing the temperature indicating the process to be endothermic. The diffusion coefficient (D) for intraparticle transport of cadmium species into the adsorbent particles has been calculated at different temperature by

$$t_{1/2} = 0.03 \times r_o^2/D \quad (20)$$

where $t_{1/2}$ is the time of half adsorption (s), r_o is the radius of the adsorbent particle (cm), D is the diffusion co-efficient in cm^2 s^{-1}. For all chemisorption system the diffusivity co-efficient should be 10^{-5}–10^{-13} cm^2 s^{-1} [43]. In the present work, D is found to be in the range of 10^{-9} cm^2 s^{-1}. The pore diffusion coefficient (D) values for various temperatures and different initial concentrations of cadmium are presented in Table 3.

To find out the energy of activation for adsorption of cadmium, the second order rate constant is expressed in Arrhenius form [44].

$$\ln k_2 = \ln k_o - E/RT \quad (21)$$

where k_o is the constant of the equation (g mg^{-1} min^{-1}), E is the energy of activation (J mol^{-1}), R is the gas constant (8.314 J mol^{-1} K^{-1}) and T is the temperature in K. Figure 5 shows that the rate constants vary with temperature according to Eq. 21. The activation energy (3.4443 kJ mol^{-1}) is calculated from slope (log k_2 vs. 1/T) of the fitted equation. The free energy change is obtained using the following relationship:

Table 3 Pore diffusion coefficients for the adsorption of cadmium at various concentrations and temperature

	Pore diffusion constant, D × 10^{-9} (cm^2 s^{-1})
Concentration (mg L^{-1})	
10	1.1771
20	0.9417
30	0.7847
40	0.6726
50	0.5885
Temperature (K)	
323	0.784
333	1.177
343	2.354

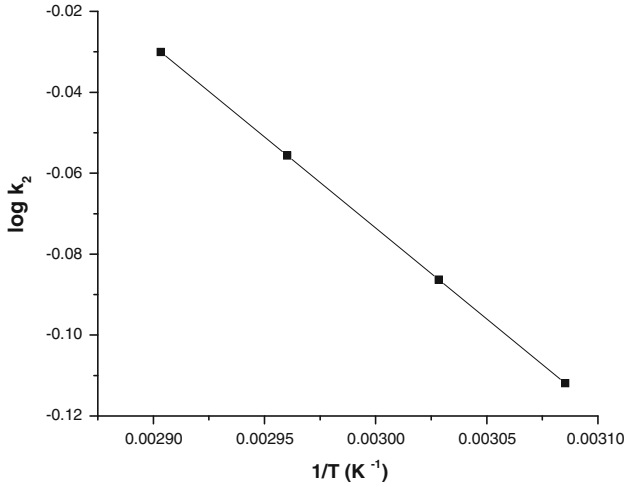

Fig. 5 Plot of log k_2 and 1/T: **a** at pH of 7.0, **b** current density of 0.2 A dm^{-2} and **c** temperature of 303 K

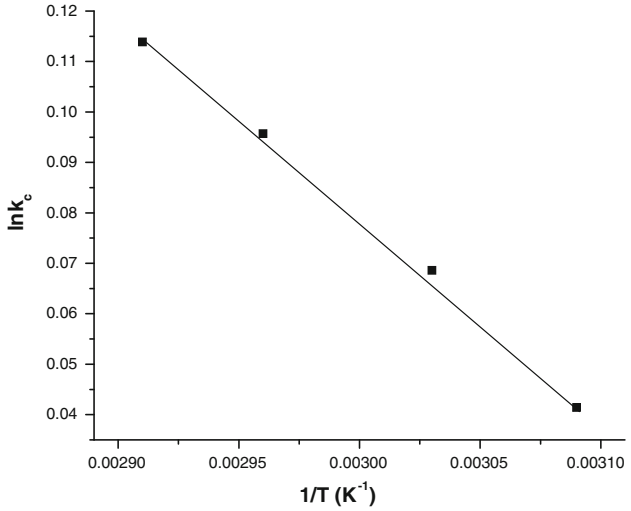

Fig. 6 Plot of ln K_c and 1/T: **a** at pH of 7.0, **b** current density of 0.2 A dm^{-2}, **c** temperature of 303 K

$$\Delta G = -RT \ln K_c \tag{22}$$

where ΔG is the free energy (kJ mol^{-1}), K_c is the equilibrium constant, R is the gas constant and T is the temperature in K. The K_c and ΔG values are presented in Table 4. From the table it is found that the negative value of ΔG indicates the spontaneous nature of adsorption.

Other thermodynamic parameters such as entropy change (ΔS) and enthalpy change (ΔH) were determined using van't Hoff equation,

$$\ln k_c = \frac{\Delta S}{R} - \frac{\Delta H}{RT} \tag{23}$$

The enthalpy change ($\Delta H = 3.2196$ kJ mol^{-1}) and entropy change ($\Delta S = 10.339$ J mol^{-1} K^{-1}) was obtained from the slope and intercept of the van't Hoff linear plots of ln K_c vs. 1/T Fig. 6. A positive value of enthalpy change (ΔH) indicates that the adsorption process is endothermic in nature, and the negative value of change in internal energy (ΔG) show the spontaneous adsorption of cadmium on the adsorbent. Positive values of entropy change show the increased randomness of the solution interface during the adsorption of cadmium on the adsorbent. Enhancement of adsorption capacity of electro coagulant (magnesium hydroxide) at higher temperatures may be attributed to the enlargement of pore size and or activation of the adsorbent surface. Using Lagergren rate equation, First order rate constants and correlation co-efficient were calculated for different temperatures (323–343 K). The calculated 'q_e' values obtained from the first order kinetics agrees with the experimental 'q_e' values better than the second order kinetics model. Table 5 depicts the computed results obtained from first and second order kinetic models. These results indicate that the adsorption follows first order kinetic model at different temperatures used in this study.

Table 4 Thermodynamic parameters for the adsorption of cadmium

Temperature (K)	K_c	$\Delta G°$ (kJ mol^{-1})	$\Delta H°$ (kJ mol^{-1})	$\Delta S°$ (J mol^{-1} K^{-1})
323	1.0422	−0.1112		
333	1.0817	−0.2126	3.2196	10.339
343	1.1206	−0.3248		

3.8 Process scale-up

On the basis of results obtained on the laboratory scale, a large capacity cell was designed, fabricated and operated for the removal of cadmium from water. The solution of 9.0 L was used for each experiment as the electrolyte. A cell [0.40 (length) × 0.30 (width) × 0.25 m (height)] was fitted with PVC cover having suitable holes to introduce anode, cathode, thermometer and the electrolyte acted as the cell. A magnesium anode [0.17 (width) × 0.18 m (height)] was used. Stainless steel plates of same dimension as that of anode were used as cathode. The cell was operated at a current density of 0.2 A dm^{-2} and the electrolyte pH of 7.0. The results showed that the maximum removal efficiency of 98.4% was achieved at a current density of 0.2 A dm^{-2} and a pH of 7 using magnesium as the anode and stainless steel as the cathode. The results were consistent with the results obtained from the laboratory scale, showing that the process was technologically feasible.

Table 5 Comparison between the experimental and calculated q_e values for the cadmium concentration of 20 mg L^{-1} in first and second order adsorption kinetics at various temperature and at pH 7

Temperature (K)	q_e (exp)	First order adsorption			Second order adsorption		
		q_e (Cal)	$K_1 \times 10^4$ (min mg^{-1})	R^2	q_e (Cal)	$K_2 \times 10^4$ (min mg^{-1})	R^2
323	19.749	15.1675	−0.00290	0.9929	19.899	0.7684	0.9991
333	19.786	15.1504	−0.00362	0.9991	19.913	0.8782	0.9992
343	19.804	15.1604	−0.0015	0.9979	19.924	0.9262	0.9996

3.9 Surface characterization

3.9.1 SEM and EDAX characterization

A SEM image of magnesium electrode after electrocoagulation of cadmium electrolyte was obtained (Fig. 7). The electrode surface is found to be rough, with a number of dents of ca. 50 μm. These dents are formed around the nucleus of the active sites where the electrode dissolution results in the production of magnesium hydroxides. The formation of a large number of dents may be attributed to the anode material consumption at active sites due to the generation of oxygen at its surface.

Energy-dispersive analysis of X-rays was used to analyze the elemental constituents of cadmium-adsorbed magnesium hydroxide shown in Fig. 8. It shows that the presence of Cd, Mg and O appears in the spectrum. EDAX analysis provides direct evidence that cadmium is adsorbed on magnesium hydroxide.

3.9.2 FTIR and XRD analysis

Figure 9 presents the FT-IR spectrum of cadmium-magnesium hydroxide. The sharp and strong peak at 3694.57 cm^{-1} is due to the (O–H) stretching vibration in the $Mg(OH)_2$ structures. The 1633.92 cm^{-1} peak indicates the bent vibration of H–O–H. A broad absorption band at 3444.38 cm^{-1} implies the transformation from free protons into a proton-conductive state in brucite. The strong peak at 458.54 cm^{-1} is assigned to the Mg–O stretching vibration [45]. The spectrum data are in good agreement with the reported data [43]. Mg–Cd is observed in –OH stretching region. Electrocoagulation-by product showed the well crystalline phase of magnesium hydroxide (Fig. 10).

4 Conclusion

The results showed that the optimized removal efficiency of 98.6% was achieved at a current density of 0.2 A dm^{-2} and pH of 7.0 using magnesium as anode and stainless steel as cathode. The magnesium hydroxide generated in the cell remove the cadmium present in the water and to reduce the cadmium concentration to less than 0.005 mg L^{-1}, and made it for drinking. The results showing that the process was technologically feasible. The adsorption of cadmium preferably fitting Langmuir adsorption isotherm better than Freundlich isotherm. The adsorption process follows second order kinetics. Temperature studies showed that adsorption was endothermic and spontaneous in nature.

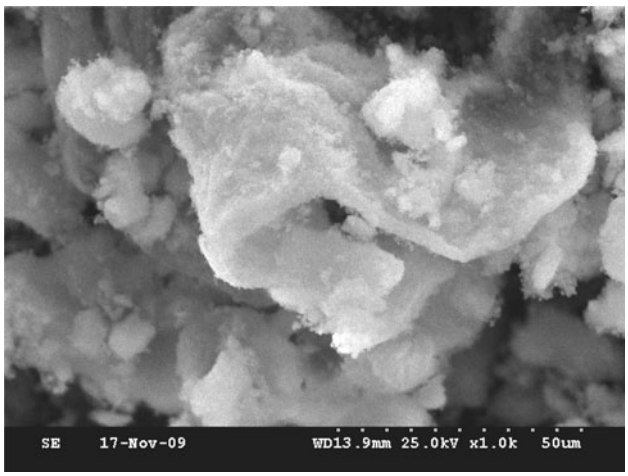

Fig. 7 SEM image of the anode after treatment

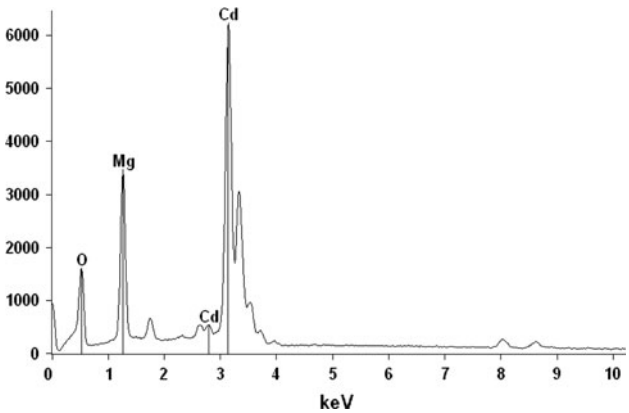

Fig. 8 EDAX spectrum of cadmium adsorbed electrocoagulant

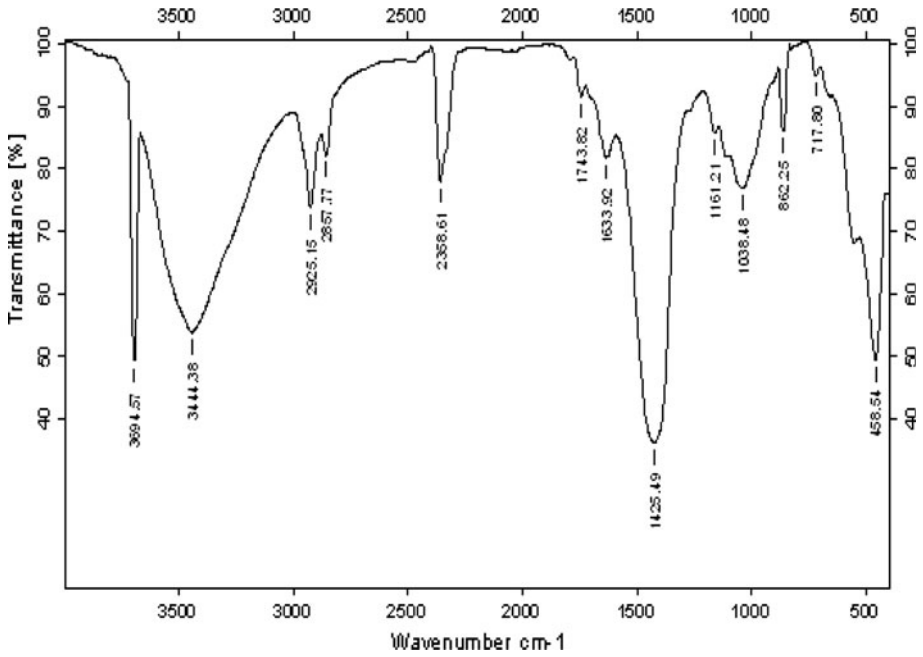

Fig. 9 FTIR spectrum of cadmium adsorbed electrocoagulant

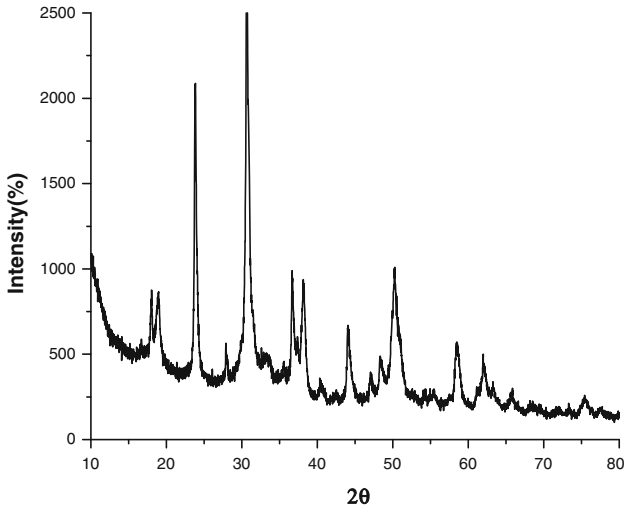

Fig. 10 XRD spectrum of cadmium adsorbed electrocoagulant

Acknowledgments The authors wish to express their gratitude to the Director, Central Electrochemical Research Institute, Karaikudi, for aid in publishing this article.

References

1. Tsezos M (2001) Hydrometallurgy 59:241
2. Sag Y, Aktay Y (2002) Biochem Eng 12:143
3. Bedow K, Bekri-Abbes I, Srasra E (2008) Desalination 223:269
4. Nogawa K, Kobayashi E, Okubo Y et al (2004) Biometals 17:581
5. Friberg L (1983) Annu Rev Public Health 4:367
6. Park S, Kim Y (2005) Mater Sci Eng 391:121
7. Sekar M, Sakthi V, Rengaraj S (2004) J Colloid Interface Sci 279:307
8. Youssef AM, Nabarawuy TE, Samra SE (2004) Colloids Surf A Physicochem Eng Asp 235:153
9. Turner MA (1983) J Environ Qual 2:118
10. Theis TL, Lyer R, Ellis SK (1992) AWWA 84:101
11. Ibrahim SC, Hanafiah MAK, Yahya MZA (2006) Am Eurasian J Agric Environ Sci 3:179
12. Megat Hanafiah MAK, Yahya MZA, Zakaria H et al (2007) J Appl Sci 7:489
13. Friberg L, Pisscator M, Nordberg G (1971) Cadmium in the environment. Chemical Rubber Co. Press, Cleveland
14. Dong D (2001) Microchem J 69:89
15. Edwards M, Benjamin MM (1989) J Water Pollut Control Fed 61:481
16. Cristophi CA, Axe L (2000) J Environ Eng 126:67
17. Na JW, Lee KJ (1993) Ann Nucl Energy 20:455
18. Sahin S (1995) Rev Roum Chim 40:157
19. Rahman MS, Islam MR (2010) Energy Sources Part A 32:222
20. Kausepediene D, Snukiskis J, Gefeniene A (1998) J Radioanal Nucl Chem 229:129
21. Jiang JQ, Xu Y, Quill K et al (2006) J Environ Chem 3:350
22. Kabay N, Arar O, Acar F et al (2008) Desalination 223:63
23. Turek M, Bandura B, Dydo P (2008) Desalination 223:17
24. Melnik L, Vysotskaja O, Kornilovich B (1999) Desalination 124:125
25. Jiang JQ, Xu Y, Simon J et al (2006) Water Sci Technol 53:73
26. Woytowich DL, Dalrymple CW, Britton MG (1993) Mar Technol Soc J 27:62
27. Chen X, Chen G, Yue PL (2002) Chem Eng Sci 57:2449
28. Jiang JQ, Graham N, André C et al (2002) Water Res 36:4064
29. Vasudevan S, Sozhan G, Ravichandran S et al (2008) Ind Eng Chem Res 47:2018
30. Malkoc E, Nuhoglu Y (2007) Sep Purif Technol 54:291
31. Namasivayam C, Ranganathan K (1995) Water Res B105:121
32. Johnson BB (1990) Environ Sci Technol 24:112
33. Izanloo H, Nassir S (2005) Iran J Environ Health Sci Eng 2:33
34. Nadhem Hamadi K, Chen XD, Mohammed Farid M, Max Lu GQ (2001) Chem Eng J 84:95
35. Archana A, Sahu KK (2006) J Hazard Mater 137:915
36. Uber FH (1985) Z Phys Chem 57:387
37. Yiacoumi S, Tien C (1995) J Colloid Interface Sci 175:333

38. Langmuir I (1918) Am Chem Soc 40:1361
39. Demiral H, Demiral I, Tumsek F, Karacbacakoglu B (2008) Chem Eng J 144:188
40. Oguz E (2005) Colloids Surf A 252:121
41. Michelson LD, Gideon PG, Pace EG, Kutal LH (1975) Office of Water Research and Technology Bulletins No 74
42. Yang XY, Al-Duri B (2001) Chem Eng J 83:15
43. Golder AK, Samantha AN, Ray S (2006) Sep Purif Technol 52:102
44. Abu-Sharara TM, Mash'Ala Y, Fayyad MK (1997) Arid Land Res Manag 11:23
45. Hernandez-Moreno MJ, Ulibarri MA, Renon JL, Serna CJ (1985) Phys Chem Miner 12:34